POLITECNICO DI TORINO
Repository ISTITUZIONALE

Autonomous detection and ascent of a step for an electric wheelchair

(Article begins on next page)

17 July 2022

Highlights

Autonomous detection and ascent of a step for an electric wheelchair

Andrea Botta, Roberto Bellincioni, Giuseppe Quaglia

- This paper addresses the problem of architectural barriers and wheelchairs

- This study proposes a method to classify a step

- This study proposes an autonomous step climbing wheelchair

- The proposed solutions were tested on an actual prototype

Autonomous detection and ascent of a step for an electric wheelchair

Andrea Botta[a,∗], Roberto Bellincioni[a], Giuseppe Quaglia[a]

[a]*Politecnico di Torino, Department of Mechanical and Aerospace Engineering - DIMEAS, Corso Duca degli Abruzzi 24, Torino, 10129, Italy*

Abstract

With the number of individuals using a wheelchair on the rise, the issue of removing architectural barriers, or at least overcoming them, has to be faced to improve independence, inclusiveness, and participation of wheelchair users. Some electric wheelchairs can climb and descend stairs and obstacles, however, the actual operations required to do so safely may be complex and may require an experienced or trained user. To overcome this issue, a method to first detect and classify a step and then autonomously climb it safely is proposed here. The same method is then applied and tested on an actual stair-climbing wheelchair prototype to prove its reliability in different conditions.

Keywords: SDG 3, Autonomous wheelchair, Stair-climbing wheelchair, Architectural barriers, Step detection

1. Introduction

The topic of eliminating architectural barriers, or at least overcoming them, is attracting increasing attention due to the rising trend of wheelchair users and their need for accessible and inclusive spaces. Worldwide, it is estimated that about 1% of the population of developed countries uses a wheelchair. In less developed countries, the percentage of people who need a wheelchair is greater than 1%, but only between 5% and 15% of these have one available [1]. It is mandatory that at least all public spaces have adequate accessibility, necessary not only for disabled people but for the entire community in order to avoid limited participation and isolation [2, 3]. In Italy, during the 2017/18 academic year, only 32% of the schools were free from architectural barriers. The most common barrier is the lack of an elevator or the presence of an elevator unsuitable for the transport of people with disabilities (63%); less frequent are schools without standard bathrooms (30%), external ramps (23%) or stairlifts (21%). In addition, there are rare cases where some stairs or doors (respectively, 7% and 4%) are not up to the standard [4].

The accessibility issue is not only limited to people with disabilities: the shift toward an increased number of older people in the population is a global phenomenon due to a decline in fertility rates, reduction of mortality rates, and increased longevity. In 2010, 10% of the global population was 60 years of age or older, but by 2050, more than 20% of the population is expected to be at least 60 years of age [5]. Farber et al. [6] discuss factors that may prevent access, inclusiveness, and participation of the elderly, similar to the ones people with disabilities may face.

Within this global scenario described above, this work also wants to contribute to the third sustainable development goal (SDG3 - Ensure healthy lives and promote well-being for all of all ages) proposed by the United Nations [7].

About 90% of all wheelchairs are manually driven [4], however, some researchers suggest that wider use of power wheelchairs could provide enhanced mobility, independence, and participation in community-based activities [8, 9]. Even if architectural barriers are a common issue for any kind of wheelchair user, electric wheelchair users are the ones who suffer the greatest effects. Manual wheelchair users generally tend to be more active, stronger, and more independent in their daily activities, in part because their wheelchairs are lightweight; on the contrary, electric powered wheelchairs are bulky and heavy, with the result that they may limit mobility even more. Also, the user visibility of the surroundings may be significantly reduced, leading to the possibility to tip over from unseen descending steps or similar obstacles or even to bump into something. For this reason, most of the state of the art regarding wheelchair overcoming obstacles is mainly focused on electric wheelchairs. Sundaram et al. [10] give a broad overview of different approaches to overcome architectural barriers, mostly stairs, in the scientific literature and available commercial solutions. Generally speaking, the most widely adopted solutions propose electric wheelchairs with tracks [11], wheels and tracks [12], or a combination of tracks, wheels, and legs [13, 14]. In the past, the authors developed an electric wheelchair for climbing stairs, called Wheelchair.q05, with an innovative hybrid locomotion unit [15–18]. In addition to its ability to climb stairs, its unique locomotion units allow the wheelchair to overcome single steps always facing the direction of motion. This prototype was later used to test the autonomous features proposed in this paper.

Whatever the locomotion unit of the wheelchair, it can be stated that these types of wheelchair are complex machines that can be fully operated by an experienced user or employing a suitable electronic controller. Given the authors experience manually operating the wheelchair proposed here, the user has to control several actuators at the same time and with some ac-

---

curacy to avoid dangerous manoeuvres. Also, for a user sitting in the wheelchair is not easy to keep monitoring the position of each moving part since the wheelchair itself obstructs his/her view, hence he/she has to control some actuators following his/her experience. On the other hand, an autonomous machine can easily control several degrees of freedom at the same time and can also monitor the state of the whole machine and its surroundings to perform such control precisely and safely. Naturally, the first step of a controller is to identify a potential obstacle before facing it properly. The literature collects several methods to achieve this task, but it is possible to identify two main approaches: vision-based estimation and range-based estimation. In the first case, a stereo-camera system is used to estimate the obstacle (i.e., a staircase or a step) by means of the detection of its distinctive features in the image [19–22]. Range-based techniques, instead, use a sensor, or an array of sensors, namely, sonars, radars and LIDARs (Light Detection And Ranging or Laser Imaging Detection and Ranging), to collect a set of measures of angles and distances that are then processed in order to estimate the geometric features of an architectural barrier [23–28]. Recently, hybrid solutions that employ RGB-D cameras to use image processing methods together with depth measures seem to be promising [29–31].

Most of the range-based techniques focus on the use of 3D scanning sensors, hence a lot of data point has to be collected to classify the obstacle correctly. Planar rangefinders instead enable to reduce considerably the size of the point cloud and still be able to properly classify the architectural barrier, by leveraging on the fact that single steps and stairs have a very distinctive profile. Alternatively, by collecting the same amount of data as in a 3D setup, it is possible to achieve planar estimation with excellent resolution. Hence, this study proposes a simple, yet effective, and successful range-based estimation of architectural barriers composed of two 360° LIDAR scanners and an effective autonomous climbing state machine based on obstacle classification outputs. A very similar approach was proposed and tested by Chocoteco et al. in [32, 33]. Compared to measuring systems based on a relatively high number of simpler range-based sensors, such as ultrasonic sensors [34] or photoelectric sensors [35], this solution enables one to achieve obstacle classification with a simpler sensor architecture with significantly fewer sensors that have to be managed without the complexity of recognising an obstacle from a 3D point cloud or from a 2D image. In particular, this paper focuses on the classification of a single step and its subsequent overcome, performed autonomously by the wheelchair. In the following section, the method to classify a step using two LIDARs is described, then a state machine for the autonomous tasks is proposed. The proposed method is then applied and tested on Wheelchair.q05, for this reason, the prototype wheelchair and its working principle are described briefly.

2. Methods

In this section, the general method of estimating significant features of an obstacle to classify it as a step or not is presented. After that, a proposal for an autonomous control system based on this method is made. A schematic description of how Wheelchair.q05 works and how it can climb or descend stairs and steps is also provided.

2.1. Single step classification

An obstacle climbing wheelchair requires to detect and measure correctly a single step in front of it in order to face it safely. Figure 1 depicts the working principle behind the proposed method. Two 360° LIDAR are fixed to the wheelchair structure, one per side, with their scanning planes parallel to the sagittal plane of the wheelchair. The user manually stops the wheelchair in front of the step and selects on the control panel the execution of the automatic step climbing sequence. The two lidar sensors begin to scan the surrounding environment, returning a cloud of points in polar coordinates from which, through some post-processing, the dimensions of the step and the relative yaw angle between the wheelchair and the step are detected. Thanks to these measurements, the wheelchair can automatically manage the approach and the overcoming phase, moving the locomotion system and the subframe of the wheelchair by the quantities necessary to overcome the step of the detected size.

Figure 2a shows how the features of the step are estimated from a LIDAR point cloud. The LIDAR sensor scans the surrounding environment to collect a reasonable number of samples of polar coordinates, namely, the distance $\vec{r}_{L_\sim}$ and the angle $\theta_{L_\sim}$, in the LIDAR reference frame $\{L_\sim\}$. Where the symbol $\sim$ stands for L and R, the left and right side, respectively. Intuitively, the potential step may be located only in a sector of the scan plane, hence only the data with angular coordinates $\theta_{L_\sim} \epsilon [0, \pi/2]$ are considered. Furthermore, all remaining points with unfeasible coordinates are discarded, namely points below the ground or much higher than the step. The point cloud is then filtered using an algorithm based on the moving average.

After the data conditioning, it is possible to begin the step classification in order to obtain 5 parameters: the distance d between the step and the wheelchair reference frame $\{P\}$, the height of the step h, the distance after the step e, the relative yaw angle γ_L and a Boolean value representing if it is feasible to climb the step or not, according to the physical characteristics of the wheelchair. The dimension d is obtained by scrolling all the points of the profile starting from the point below the LIDAR ($\theta_{L_\sim} = \pi/2$) and verifying when one of them presents a value of the ordinate $y_{L_\sim}$ that is outside a confidence region centred on the ground with a width of $2\varepsilon_d$, a value that mainly depends on the LIDAR accuracy, i.e. when $y_{L_\sim} < H_{L_\sim} - \varepsilon_d$, it is possible to state that there is a vertical surface. The ordinate $y_{L_\sim}$ of the point, called *Mark1*, is the distance d. In order to estimate the step height h, a similar approach is used. Starting from *Mark1*, the first point, called *Mark2*, outside a new confidence region centred around $x_{L_\sim, Mark1}$ with a width of $2\varepsilon_h$ can be considered part of a horizontal surface following the step. The step height is then given by $h = H_{L_\sim} - y_{L_\sim, Mark2}$. Similarly to the distance d, the estimate of how much space there is after the step, the value e, is given by the difference $e = x_{L_\sim, Mark3} - x_{L_\sim, Mark1}$, where *Mark3* is the last point or a point where starts another
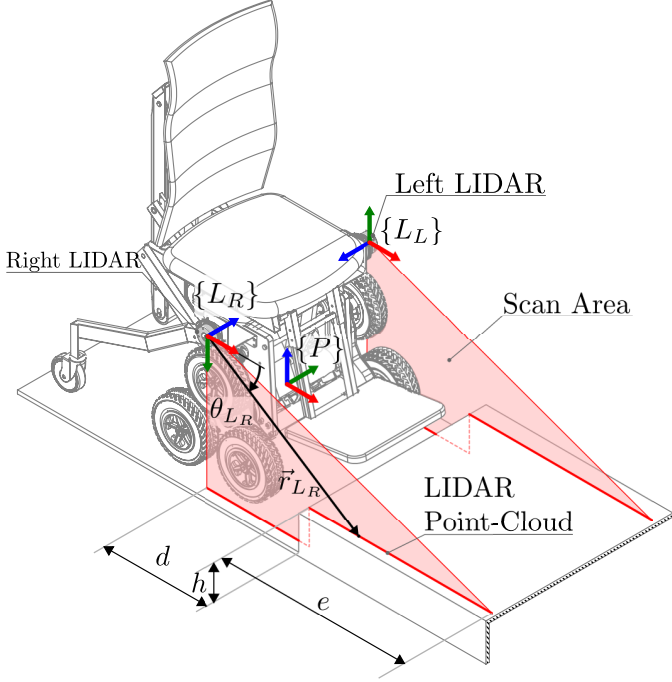
Figure 1: Single step classification working principle

Figure 2: Single step features estimation. (a) Side view. (b) Top view with relative rotation between the wheelchair and the step.

vertical surface, like for *Mark1*. The relative yaw angle γ_L (Figure 2b) is computed from the estimates d_L and d_R as follows

$$\gamma_L = \tan^{-1} \frac{d_R - d_L}{i} \tag{1}$$

where i is the distance along $\hat{y}_{\{P\}}$ between the two LIDAR reference frames.

By knowing all these estimates, it is possible to check if the wheelchair is able or not to climb the step.

2.2. Single step climbing control

The classifying method described before becomes the core element of the state machine governing the autonomous surpassing of a step. Figure 3 depicts a schematic representation of the proposed state machine. When the user faces an architectural barrier like a sidewalk or a single step, he/she can activate the autonomous sequence to climb. First, several LIDAR scans are collected and processed as described above. The results of the single step classification (i.e., d, h, e, γ_L and a Boolean feasibility value) are then used to distinguish between three possible outcomes. If the controller determines that the wheelchair cannot surpass the obstacle, for whatever reason, it goes back to the idle state, waiting for the user to take control back. Conversely, if a feasible step is detected, two different behaviours are activated depending on the value of d. If d is large (the actual threshold depends on the LIDAR accuracy), the wheelchair automatically moves closer to the step and compensates for the relative rotation γ_L and then returns to the step classification procedure in order to improve its estimate. If instead, the wheelchair is sufficiently close to the step, both after the first scan or after the second one, the complete autonomous sequence to climb the step is activated.
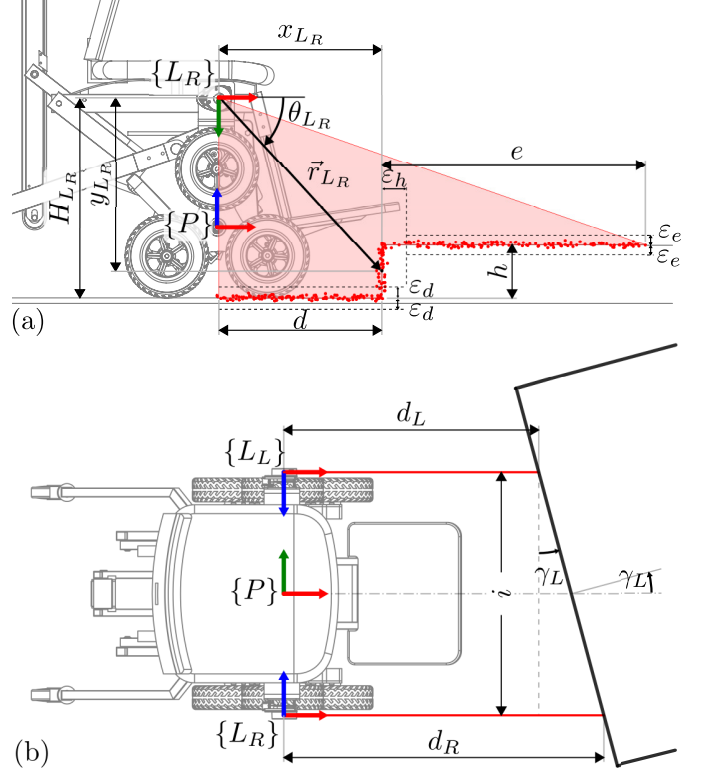
The actual autonomous sequence is strictly related to the wheelchair features, but generally speaking, both the LIDAR estimated parameters and potentially other information from other sensors are used to generate the required reference for the closed loop control system of the actuators. In the following, an example of an autonomous sequence, based on the wheelchair used for the tests, is briefly described.

2.3. Wheelchair.q05 working principle

The methodology discussed previously is general and could work for any stair-climbing wheelchair. The proposed methodology was tested using a prototype of a stair-climbing electric wheelchair, named Wheelchair.q05, developed at Politecnico di Torino.

As detailed in Figure 4, Wheelchair.q05 is composed of 5 main subsystems. All elements are fixed to the main chassis PCD; Θ_{PC} is the absolute inclination of the chassis with respect to the world reference frame. A revolute joint in C enables a relative rotation β between the fixed chassis and the mobile one (CRE) with the main function of tilting the wheelchair seat, mounted on the mobile chassis, by an angle Θ_{CR} about the world reference frame. The link ES rotates of an angle θ_{ES} around the revolute joint in E to deploy an idle track that is free to rotate around S. The track provides an adequate number of contact points with at least three steps of a stair to guarantee wheelchair stability. When in driving mode or facing a single step, the track is not required, therefore, it is in its retracted position. A set of two pivot wheels is mounted at the end of the

link DU. This link rotates by an angle θ_{DU} about the revolute joint in D in order to improve user comfort in various situations, but also to shift back and forth the wheelchair centre of mass location in a controlled manner to maintain always static stability. The locomotion unit is composed of a triangular shaped epicyclical gearing mechanism that can rotate of an angle θ_P about P.

Figure 5 depicts with more detail how the hybrid leg-wheel locomotion unit works. The arms of the tripod constitute the planet carrier of an epicyclical mechanism in which the central solar gear transmits the motion to the wheels coupled with the 2nd planet gears by means of three idle planet gears (a). Hence, each locomotion unit has two degrees of freedom (d.o.f.): the rotation of the wheels relative to the carrier ω_{Wheel}, and the revolution θ_P ($\dot{\theta}_P = \Omega_{Carrier}$) of the carrier with respect to the fixed chassis PCD. To ensure safety and complete control of the machine, both d.o.f.s are actuated. In particular, two DC gear motors, one per side, drive the solar gears, while a single DC motor actuates both carriers synchronously. By combining the motors rotations, the wheelchair can both drive and overcome architectural barriers (b). In particular, the figure represents the two most useful cases: in the first and last parts, the carrier rotation is locked, and the unit is in "driving mode"; while climbing or descending a step, instead, the sun gear spins to compensate the wheels rotation induced by the carrier revolution, this results in a revolution of the carrier with locked wheels.

2.4. Wheelchair.q05 autonomous climbing sequence

As mentioned before, the actual autonomous climbing sequence strictly depends on the wheelchair itself. In particular, for Wheelchair.q05, the step climbing sequence consists of the following phases:

- **A0**: The wheelchair uses the estimated distance d and the relative orientation γ to begin the approach to the step based on the inverse kinematics of a differential drive robot. At the same time, the tripods (the carriers of the epicyclical mechanism) rotate to lift the most upfront wheels above the step of height h. The wheelchair slows down as travels closer to the step, but it keeps gently driving toward the step until both the wheels on the ground touch it and a torque spike is measured employing current sensors. The latter is an additional safety measure to compensate small estimation errors, both for d and for γ_L.

- **A1**: The locomotion motors spins to keep the wheels locked in place while the tripods rotate to let the lifted front wheels touch the step top surface. During this phase, the rear pivoting wheel deployment mechanism maintains the required wheelchair inclination.

- **A2**: The tripods rotations lift the wheels on the ground at the same height as the front ones. The actuation of the pivoting wheels keeps the wheelchair level.

- **A3**: The wheelchair advances until the rear wheels of the tripods have a sufficiently large clearance from the edge of the step.

- **A4**: The pivoting wheels and the tripods move at the same time to tilt the wheelchair forward to shift its whole weight to the tripod wheels in contact with the ground.

- **A5**: The wheelchair is statically balanced on the tripods wheels; hence the pivoting wheels are lifted just a little above the height h.

- **A6**: The wheelchair advances until a safety margin is obtained between the pivoting wheels and the edge of the step.

- **A7**: The tripods and the pivoting wheels are positioned in the default configuration for navigation. The autonomous sequence is completed.

The entire sequence takes place without user intervention. The actuators are governed by closed-loop position control systems that use the transducers on the wheelchair to generate feedback signals to be compared with the signals sent. The transition from one phase of the sequence to the next occurs when the kinematic elements of the wheelchair have reached the correct positions and the conditions for the transition to the next action have been met.

3. Results

This section briefly summarises the experimental setup used to test the autonomous climbing sequence, and then some insights about the experimental results are given.

3.1. Experimental setup

The following setup was used to perform the tests (Figure 6). A wooden platform of fixed plant dimensions (1500×1500 mm) and adjustable height (it can be set to $68\tilde{\text{m}}$m or 90 mm) was placed in front of Wheelchair.q05 to act as the architectural barrier. Wheelchair.q05 has dimensions comparable to a typical electric wheelchair (about $0.7 \times 1.2 \times 1.3$ m with a mass of 80 kg). A Speedgoat education real-time target machine (Speedgoat GmbH, Liebefeld, Switzerland) is employed as the main controller of the wheelchair, hence the whole state machine governing Wheelchair.q5 was designed with Simulink (The Mathworks Inc., Natick, MA). The real-time machine is equipped with a proprietary input/output board (IO102) with 32 single-ended (or 16 differential) analog inputs with a resolution of 16 bit over the ± 10 V range, 16 digital (TTL) inputs, and 4 single-ended analog outputs with a resolution of 16 bit over the ± 10 V range. The data filtering of the acquired signals is done via software by employing the moving average algorithm. The sampling frequency and the controller frequency are both 1 kHz. The LIDAR sensor (RPLIDAR A1M1-R1, Shanghai Slamtec Co. Ltd., China) is mounted on the chassis CDP using a 3D printed support. The support fixes the sensor reference frame $L_\sim$ in a known position with respect to P in order to be able to apply a geometric transformation to the measurement in a more suitable reference frame. When Wheelchair.q05 is in its default configuration on flat ground, the xz plane defined by $L_\sim$ is parallel to the ground, the plane yz contains the point P,
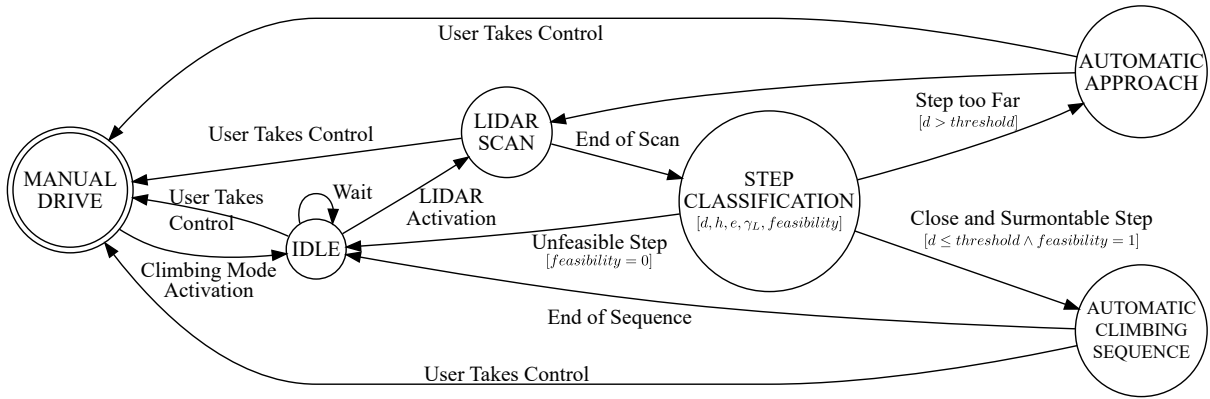
Figure 3: Autonomous step classification and climbing state machine
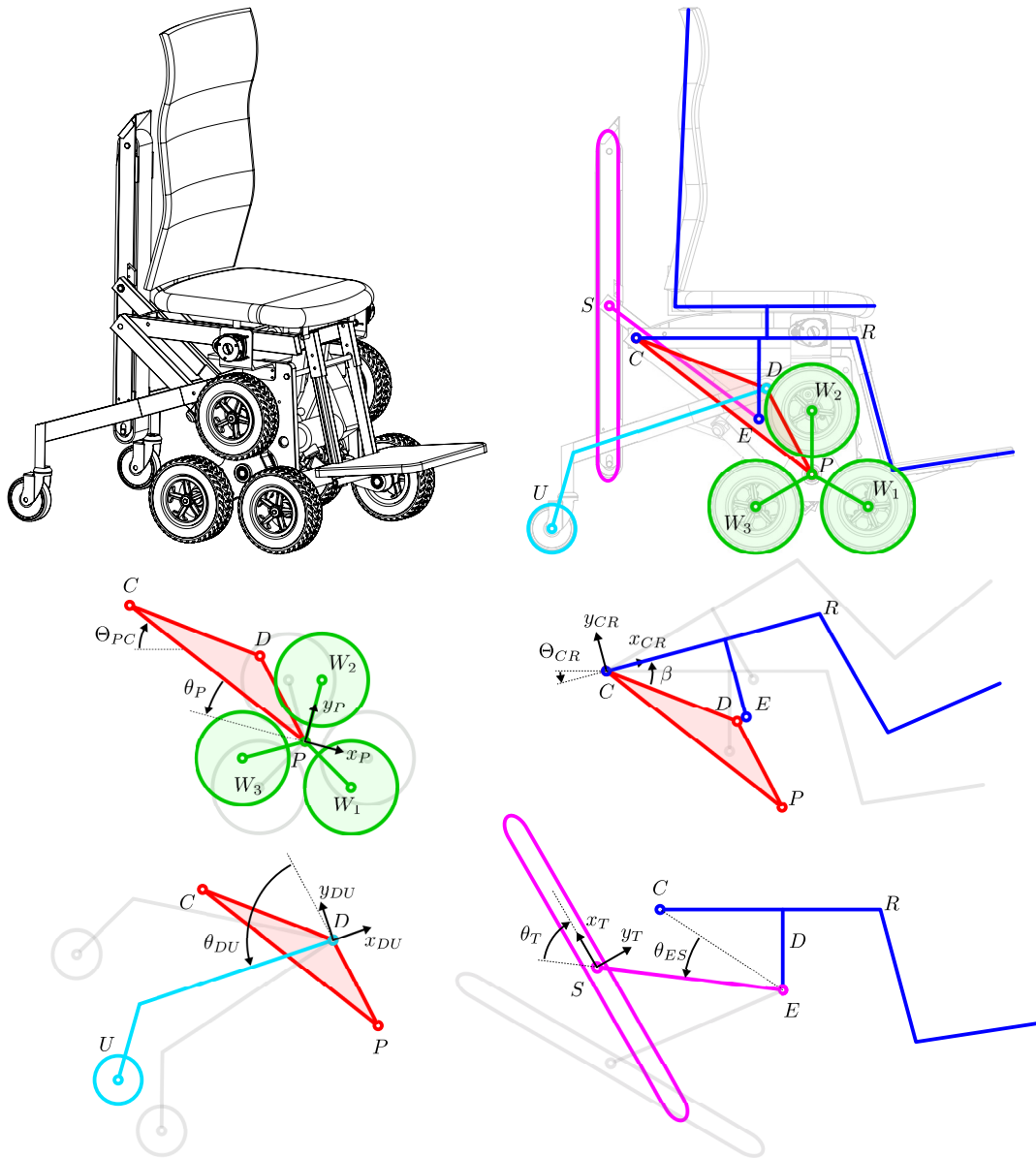

Figure 4: Wheelchair.q05 functional scheme of its main components. In red the fixed chassis *PCD*, in blue the mobile chassis *CRE*, in green the locomotion unit, in cyan the pivot wheels and in magenta the idle track
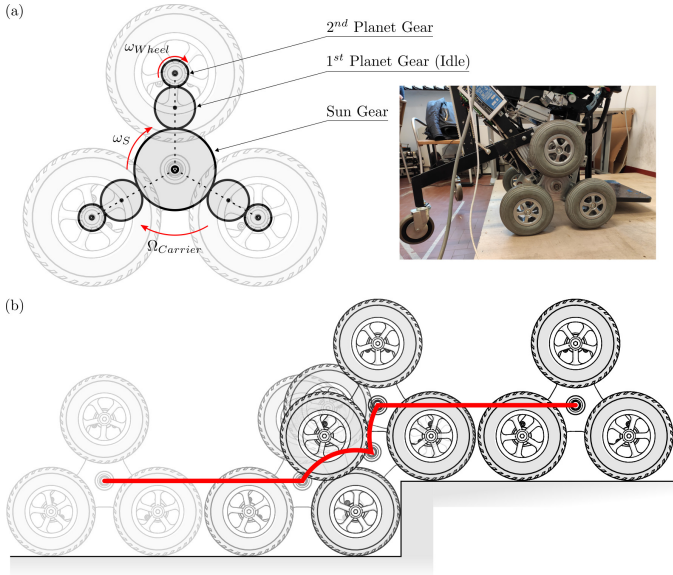
Figure 5: (a) Wheelchair.q05 locomotion unit functional scheme. (b) Locomotion unit sequence while facing a single step.

the plane xy is 46 mm beyond the wheels external face, the axis $\hat{x}_{\{L_\sim\}}$ points forward and $\hat{x}_{\{L_\sim\}}$ points inward, and the LIDAR centre is placed about 800 mm above ground.
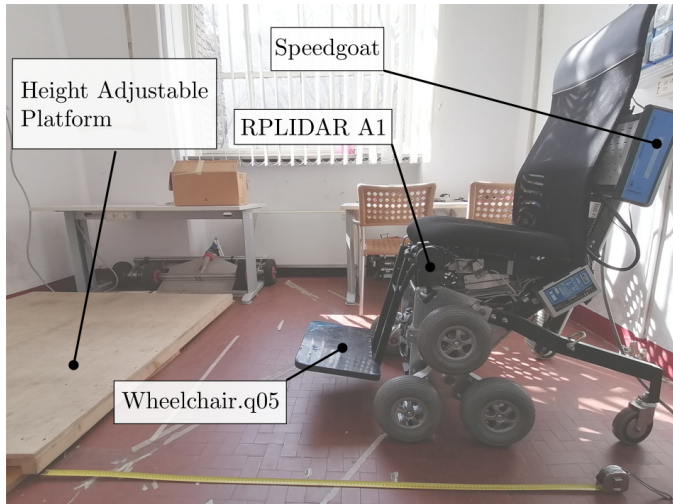

Figure 6: Experimental setup

All preliminary tests were done without a user in the wheelchair for safety reasons. Hence, Wheelchair.q05 is remotely controlled both to set the initial position, to start the autonomous mode, and to switch from the automatic sequence to manual drive whenever the user wants to regain control. Future tests are going to use a dummy to comply more appropriately with the wheelchair testing standards defined in ISO 7176.

3.2. Experimental results

3.2.1. Step classification

Table 1 provides an overview of some of the experimental classification tests. The wheelchair was positioned in front of a

wooden platform, representing a step, of known dimensions and distance from the wheelchair. The distance from the LIDAR to the step edge is often slightly overestimated, for this reason, the automatic sequence uses an auxiliary method to check the distance from the step edge, namely locomotion motors currents monitor to sense contact. In particular, the wheelchair keeps advancing very gently until it bumps against the curb, when a bump is detected by measuring a current spike in a traction motor, that side stops while the other keeps going until it makes contact with the step. The latter is a yaw rotation in place of the whole wheelchair about the contact point of the first wheel that has bumped. A more elegant and contactless solution could be re-orienting the ultrasonic range finder to point forward to make an analogous safety check. The step height is generally the best estimate with a very limited error. On the other hand, the estimation of how much space is available beyond the step edge presents a quite evident overshoot. This is the main reason why there are two LIDAR scans if the automatic sequence is enabled beyond a threshold distance: the first scan is used to control an initial approach to the step to then do a second scan that estimates the step dimensions.

Figure 7 shows the step classification process in more detail in an example of the step classification done with a single LIDAR mounted on the left side of Wheelchair.q05. The top figure shows a sector of the raw LIDAR scan and the post-processed scan. Raw scans are quite noisy; however, the post-processing is reliable enough to obtain a clear step profile in a wide range of test scenarios. From the post-processed data, the step classification is performed, as described before, by means of 3 key points (*Mark1*, *Mark2*, and *Mark3*). The bottom figure highlights these points and shows the estimation results. The distance d is estimated with an error of -0.64%, the height h with an error of 0.27%, and the distance e with an error of 22.33%. On average, instead, the distance d is estimated with an error of 3.37%, the height h with an error of 0.89%, and the distance e with an error of 19.64%
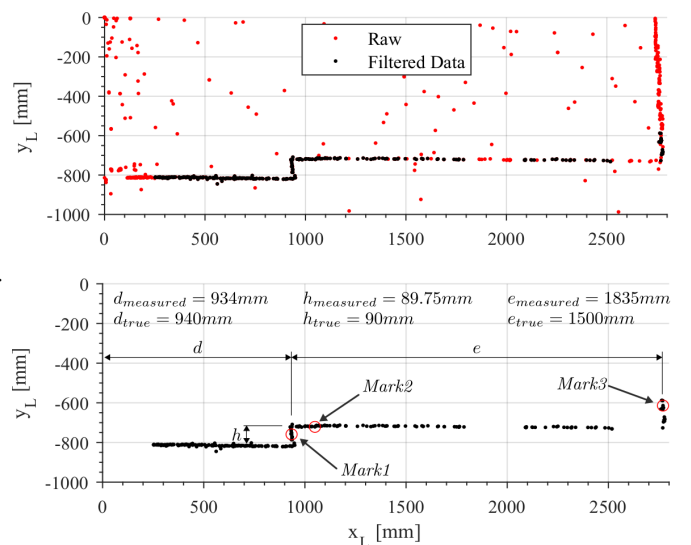

Figure 7: Experimental Step Classification. Top figure shows raw and post-processed LIDAR data in $\{L_L\}$. Bottom figure shows the classification results

Table 1: Step classification experimental tests

test number	d_{true} [mm]	d_{meas} [mm]	Error $\frac{d_{meas}-d_{true}}{d_{true}}$	h_{true} [mm]	h_{meas} [mm]	Error $\frac{h_{meas}-h_{true}}{h_{true}}$	e_{true} [mm]	e_{meas} [mm]	Error $\frac{e_{meas}-e_{true}}{e_{true}}$
1	500	500	0%	68	69	1.5%	1500	1816	21%
2	690	714	3.4%	68	67	-1.5%	1500	1800	20%
3	600	658	9.6%	68	63	-7.3%	1500	1810	20.6%
4	600	568	-5.3%	68	72	5.9%	1500	1695	13%
5	600	681	13.5%	90	98	8.8%	1500	1784	18.9%
6	681	712	4.5%	90	92	2.2%	1500	1802	20%
7	500	510	1.9%	90	88	-2.2%	1500	1820	21.3%
8	940	934	-0.64%	90	89	-0.27%	1500	1835	22.3%

3.2.2. Autonomous sequence

Figure 8 depicts the evolution of the reference signals generated by the autonomous control based on the classification results and how the actuators are controlled to reach these references by means of PID (Proportional Integral and Derivative) controllers tuned to obtain a safe and reliable climbing sequence. In particular, the figure shows the three main motions required to climb, namely, the two d.o.f.s of the locomotion units and the deployment mechanism of the pivot wheels.
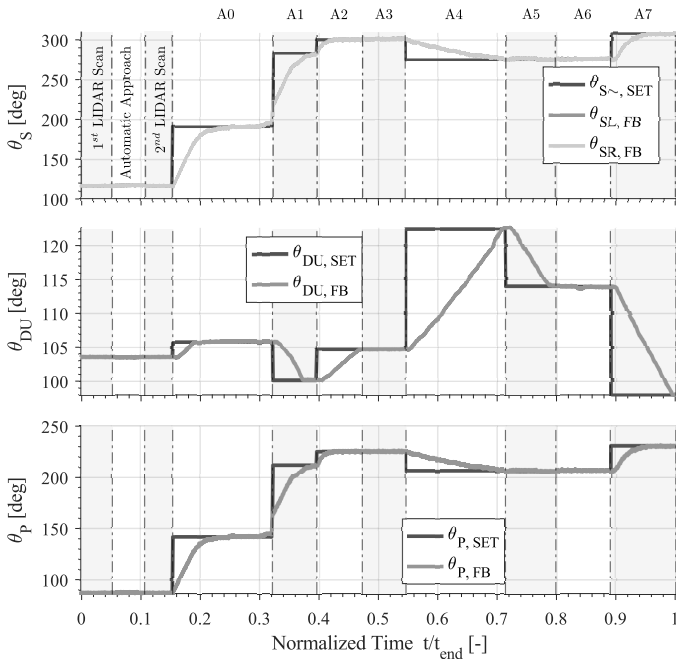

Figure 8: Reference (SET) and feedback (FB) signals of the rotation θ_S of the sun gears, angle θ_{DU} of the pivot wheels deployment mechanism, and the rotation θ_P of the carriers during the complete autonomous sequence

The sequence starts with a LIDAR scan while Wheelchair.q05 is stationary. Then, since the wheelchair is not close enough to the step, the solar gears are actuated to advance (the required rotation is minimal) to repeat the second scan used to classify the step. From this point on, the wheelchair follows the sequence of actions from A0 to A7 previously presented, where every change in any reference signal represents a transition to the next phase. The solar gears and the carrier cooperate for almost the whole sequence except when a simple advancement

is commanded (e.g., during the initial approach, A3, and A6) and therefore just the solar gears must be actuated.

Various completion times were achieved because these tests were also used to optimise the motors controllers parameters to balance the requirement of speed, effectiveness and safety. Initially, the completion time was less than 2 minutes for a complete test with a first laser scan at distance, then an approach to the step to improve the classification with a second scan, and then the complete autonomous sequence. After all tests, the same sequence lasted about 55 s.

As already said, the controllers have been initially designed with safety and reliability as the first concerns. For this reason, the actuators are far from being close to actual capabilities, and this can be seen in the longer phases, A0 and A4. A0 is clearly divided in two moments: in the first one, the carriers rotate while the wheelchair advances very slowly; then in the second moment, when the carrier rotation is complete, Wheelchair.q05 keeps advancing more quickly since the rotation of the solar gear is no more influenced by the carriers. This phase could be sped up by designing more aggressive solar gears controllers to shorten the initial and slower part. A4, instead, is a slow phase for a reason more related to safety and stability. During this phase, the centre of mass of the wheelchair is shifted forward in order to lift the pivot wheels from the ground and to balance the wheelchair only on the locomotion units wheels (two per side). Therefore, to avoid approaching this critical condition too fast, the automatic phase execution is slowed down.

4. Discussion

This section provides a brief summary of the benefits of the proposed idea, its limitations and issues, and possible solutions to address them. For better clarity, this discussion section mirrors the structure of the previous one.

4.1. Step classification

The results presented previously clearly show that the accuracy of the geometric features of the steps is particularly affected by noise over larger distances. The problem was expected but to a lesser extent. More in general, the raw sensor data appears to be much noisier when acquired with Speedgoat compared to the initial tests done with the LIDAR directly

connected to a PC. The authors' hypothesis is that the additional longer wiring and the conversion between serial protocols (UART to RS232) required by Speedgoat contribute to the noise. The issue could be mitigated by employing a LIDAR with better performance over long-range distances or by improving the signal-to-noise ratio of the current solution by improving the available hardware.

On the other hand, the most critical features of a step, namely the distance d from it and the step height h, are always estimated with significant precision. The slight deviation is easily compensated by the auxiliary checks done by the controller to verify if there is a contact or not between the wheels and the step. If desired, the LIDAR could be fixed higher on the chassis to obtain a better perspective to estimate the distance e, however, by doing so, the perspective could be not suited for estimating the step height h with the same quality.

Despite the problems, the step classification system proves to be robust during the entire experimental campaign. However, more research needs to be done on environmental factors that could affect sensor measures. In particular, this system has to be tested with steps made of different materials and with different lighting and weather conditions to evaluate how reflection, visibility, and light affect the measure. This open point is crucial to guarantee the same robustness achieved in a controlled laboratory environment, also in environmental conditions closer to real scenarios.

Beside being developed completely independently, the proposed method is very similar to the one suggested in [32]. Both methods follow a natural and intuitive procedure of aggregating the profile of obstacles measured by laser scanners into horizontal and vertical segments in order to extrapolate their geometric characteristics. In particular, both approaches use some threshold values (e.g. thresholds ε_d, ε_h, and ε_e) to define whether a point is within a group or not. The solution proposed here does not explicitly define the groupings, but it uses the significant points *Mark1*, *Mark2*, and *Mark3*. Then from each group, a geometric feature is extrapolated: in [1] the median of the relevant quantities is computed, while in this approach, the relevant values of *Mark1*, *Mark2*, and *Mark3* are considered since the data had already been filtered thoroughly.

While the concept behind the two methods is similar with some implementation differences, the method suggested here has some other minor differences. First of all, in [32] the laser sensors can scan a limited sector of the corresponding planes, thus the wheelchair must be in a predefined configuration to properly scan the obstacle. By employing a 2D laser scanner mounted in a known position instead, it is always possible to scan a relevant sector of the measuring plane in any wheelchair configuration because the homogeneous transformation between the reference frames $\{L_\sim\}$ and $\{P\}$ allows one to properly interpret the data in any configuration. Furthermore, the approach proposed and tested in [32, 33] required and implemented two laser sensors, one per side. By contrast, the experimental evidence of the hereby presented method have proved that a single LIDAR is enough to estimate and overcome the obstacle if some auxiliary sensors are employed. Consequently, the proposed setup proved to be robust to the failure of the second LIDAR.

Contrary to Chocoteco et al. [32] results that could achieve an estimation error of about 2-3 mm, the implemented experimental setup was able to achieve similar results estimating h, while d and e were estimated with significant larger errors (Table 1). However, the results shown here proved to be considerably affected by the distance from the step and by noise compared to [32], where these kinds of issues were not reported. This behaviour led to developing a robust system that can compensate uncertainty and user misuse by employing the autonomous approach phase to improve estimates from far away and torque sensors to properly compensate for any γ_L.

4.2. Autonomous sequence

The autonomous sequence proves to work perfectly in every test run safely and without any problem. Future work will focus on improving this solid foundation.

The step reference signals employed to drive the autonomous sequence could be improved with smooth and synchronised reference signals of relevant motions in order to optimise user comfort during the ride. For example, during the step climb or descent, the wheelchair follows a trajectory with an evident discontinuity, therefore its actuators (in particular the one orientating the seat) could work synchronously to this trajectory to let the user centre of mass following a straight path, or at least a path without discontinuities.

Additional sensors, in particular sensors useful to estimate the wheelchair user mass and position, could be very useful to complete this phase quicker but also safer. Also, auxiliary contactless sensors to perform fine measurements and safety checks, such as ultrasonic or infrared proximity sensors, could be implemented to replace the contact-based sensors used here.

At the moment, this autonomous sequence relies on the user activating it when the path in front of the wheelchair is clear. However, if the user activates the sequence despite there being an obstacle, the two LIDARs should detect something that they cannot classify as a step, therefore the autonomous sequence does not start. As a safety feature, it is sufficient that one of the LIDARs detects an unfeasible step to go back to manual drive mode. However, the same feature could interfere with proper operation when a false negative occurs and a step is classified as unfeasible by one or both LIDARs. Also, some issue could occur if the obstacle is not in the scanned planes, in that case only the user can intervene to avoid a collision. In this scenario, it could be possible to implement some range-finder sensors pointing forward to avoid collision with un-detected obstacles.

During the autonomous phases, the user has (almost) always the possibility to switch to manual control. He/she can do it by pressing the e-stop button that halts all the motors, then removing the e-stop switch to go back to the manual drive mode, aborting the automatic sequence. As an alternative, the user can directly switch to manual drive mode without drive mode. The only instance in which the user cannot instantly switch to the manual mode is during the phase when the pivoting wheels are lifted and the wheelchair is balanced on the tripods wheels only. Even if the wheelchair is stable, it is safer to let the machine

8

complete this phase than letting the user take control because it is possible to manually force some motion that could imperil the user.

5. Conclusions

This study has proposed a simple yet reliable method to classify an ascending step (or a similar architectural barrier) in order to let an electric stair-climbing wheelchair performs an autonomous sequence to overcome it. The proposed method was then tested on an actual prototype in a wide range of experimental setups, and it proved to be a reliable solution.

Compared to other solutions, the step classification system proves to be a trade-off between effectiveness, architecture complexity, and ease of measured quantities interpretation. Yet, it proves to be a solid and reliable solution with some flaws about signal noise that can be solved by improving the proposed setup.

The experimental validation has proved that by combining simple obstacle classification methods and a robust autonomous control on an electric wheelchair properly designed to be always statically stable during its operation, it is possible to efficiently complete very complex tasks where safety is key. Therefore, the step classification will be improved in order to classify all possible architectural barriers that the wheelchair can face (e.g., ascending and descending stairs and single steps) to completely automate these complex operations.

CRediT authorship contribution statement

Andrea Botta: Methodology, Investigation, Data curation, Visualization, Writing - Original Draft, Writing - review & editing. **Roberto Bellincioni:** Methodology, Investigation, Software, Data Curation, Writing - Original Draft, Writing - review & editing. **Giuseppe Quaglia:** Writing - review & editing, Resources, Supervision, Project administration.

Declaration of Competing Interest

The authors declare that they have no known competing financial interests or personal relationships that could have appeared to influence the work reported in this paper.

References

[1] G. Emmer, Wheelchair statistics: How many wheelchair users are there? (2009).
URL https://www.newdisability.com/wheelchairstatistics.htm

[2] S. Goldsmith, Designing for the disabled: the new paradigm, Routledge, 2012.

[3] D. M. Cruz, M. L. G. Emmel, M. G. Manzini, P. V. Braga Mendes, Assistive Technology Accessibility and Abandonment: Challenges for Occupational Therapists, The Open Journal of Occupational Therapy 4 (1) (Jan. 2016). doi:10.15453/2168-6408.1166.

[4] F. Pinna, C. Garau, F. Maltinti, M. Coni, Beyond Architectural Barriers: Building a Bridge Between Disability and Universal Design, in: Computational Science and Its Applications – ICCSA 2020, Vol. 12255, Springer International Publishing, Cham, 2020, pp. 706–721. doi:10.1007/978-3-030-58820-5_51.

[5] F. Kong, Aging Trend of the World, in: T. Hoshi, S. Kodama (Eds.), The Structure of Healthy Life Determinants, Vol. 18, Springer Singapore, Singapore, 2018, pp. 7–21, series Title: International Perspectives on Aging. doi:10.1007/978-981-10-6629-0_2.

[6] N. Farber, National Conference of State Legislatures, Public Policy Institute (American Association of Retired Persons), Aging in place: a state survey of livability policies and practices, National Conference of State Legislatures ; AARP Public Policy Institute, Denver; Washington, DC, 2011, oCLC: 1015574932.

[7] Sustainable development goal 3 - department of economic and social affairs (2016).
URL https://sdgs.un.org/goals/goal3

[8] S. Evans, A. O. Frank, C. Neophytou, L. de Souza, Older adults' use of, and satisfaction with, electric powered indoor/outdoor wheelchairs, Age and Ageing 36 (4) (2007) 431–435. doi:10.1093/ageing/afm034.

[9] E. M. Giesbrecht, J. D. Ripat, A. O. Quanbury, J. E. Cooper, Participation in community-based activities of daily living: Comparison of a pushrim-activated, power-assisted wheelchair and a power wheelchair, Disability and Rehabilitation: Assistive Technology 4 (3) (2009) 198–207. doi:10.1080/17483100802543205.

[10] S. A. Sundaram, H. Wang, D. Ding, R. A. Cooper, Step-Climbing Power Wheelchairs: A Literature Review, Topics in Spinal Cord Injury Rehabilitation 23 (2) (2017) 98–109. doi:10.1310/sci2302-98.

[11] Wheelchair for Stairs Electric Climber for Disabled | Caterwil (2021).
URL https://caterwil.com/

[12] Scewo bro: independently balancing and stair-climbing wheelchair (2021).
URL https://www.scewo.ch/en/bro/

[13] M. Hinderer, P. Friedrich, B. Wolf, An autonomous stair-climbing wheelchair, Robotics and Autonomous Systems 94 (2017) 219–225. doi:10.1016/j.robot.2017.04.015.

[14] K. Sasaki, Y. Eguchi, K. Suzuki, Stair-climbing wheelchair with lever propulsion control of rotary legs, Advanced Robotics 34 (12) (2020) 802–813. doi:10.1080/01691864.2020.1757505.

[15] G. Quaglia, W. Franco, M. Nisi, Kinematic analysis of an electric stair-climbing wheelchair, Ingenieria y Universidad 21 (Dec. 2016). doi:10.11144/Javeriana.iyu21-1.kaes.

[16] G. Quaglia, M. Nisi, W. Franco, Wheelchair.q05 Final Design: An Innovative Stair-Climbing Wheelchair, in: ASME 2017 International Mechanical Engineering Congress and Exposition, American Society of Mechanical Engineers, Tampa, Florida, USA, 2017, p. V04AT05A056. doi:10.1115/IMECE2017-70750.

[17] G. Quaglia, W. Franco, M. Nisi, Analysis of the Static Stability for an Electric Stair-Climbing Wheelchair, in: Advances in Robot Design and Intelligent Control, Vol. 540, Springer International Publishing, Cham, 2017, pp. 465–473. doi:10.1007/978-3-319-49058-8_50.

[18] G. Quaglia, W. Franco, M. Nisi, Stair-Climbing Wheelchair.q05: From the Concept to the Prototype, in: Advances in Service and Industrial Robotics, Vol. 67, Springer International Publishing, Cham, 2019, pp. 245–255, series Title: Mechanisms and Machine Science. doi:10.1007/978-3-030-00232-9_25.

[19] A. Ciobanu, A. Morar, F. Moldoveanu, L. Petrescu, O. Ferche, A. Moldoveanu, Real-Time Indoor Staircase Detection on Mobile Devices, in: 2017 21st International Conference on Control Systems and Computer Science (CSCS), IEEE, Bucharest, Romania, 2017, pp. 287–293. doi:10.1109/CSCS.2017.46.

[20] D. Aguilera-Castro, M. Neira-Carcamo, C. Aguilera-Carrasco, L. Vera-Quiroga, Stairs recognition using stereo vision-based algorithm in NAO robot, in: 2017 CHILEAN Conference on Electrical, Electronics Engineering, Information and Communication Technologies (CHILECON), IEEE, Pucon, 2017, pp. 1–6. doi:10.1109/CHILECON.2017.8229674.

[21] X. Zhao, W. Chen, X. Yan, J. Wang, X. Wu, Real-Time Stairs Geometric Parameters Estimation for Lower Limb Rehabilitation Exoskeleton, in: 2018 Chinese Control And Decision Conference (CCDC), IEEE, Shenyang, China, 2018, pp. 5018–5023. doi:10.1109/CCDC.2018.8408001.

[22] M. Khaliluzzaman, K. Deb, Stairways detection based on approach evaluation and vertical vanishing point, International Journal of Computational Vision and Robotics 8 (2) (2018) 168. doi:10.1504/IJCVR.2018.091984.

[23] C. Stahlschmidt, S. von Camen, A. Gavriilidis, A. Kummert, Descending step classification using time-of-flight sensor data, in: 2015 IEEE Intel-

ligent Vehicles Symposium (IV), IEEE, Seoul, South Korea, 2015, pp. 362–367. doi:10.1109/IVS.2015.7225712.

[24] C. Stahlschmidt, A. Gavriilidis, A. Kummert, Classification of ascending steps and stairs using Time-of-Flight sensor data, in: 2015 IEEE 9th International Workshop on Multidimensional (nD) Systems (nDS), IEEE, Vila Real, Portugal, 2015, pp. 1–6. doi:10.1109/NDS.2015.7332643.

[25] H. Taniue, J. Kaneko, K. Kojima, Development of automatic barrier detection system for wheelchair, in: 2015 IEEE 4th Global Conference on Consumer Electronics (GCCE), 2015, pp. 374–376. doi:10.1109/GCCE.2015.7398730.

[26] J. Razavi, T. Shinta, A novel method of detecting stairs for the blind, in: 2017 IEEE Conference on Wireless Sensors (ICWiSe), IEEE, Miri, Malaysia, 2017, pp. 1–5. doi:10.1109/ICWISE.2017.8267155.

[27] S. Ponnada, S. Yarramalle, M. R. T. V., A Hybrid Approach for Identification of Manhole and Staircase to Assist Visually Challenged, IEEE Access 6 (2018) 41013–41022. doi:10.1109/ACCESS.2018.2852723.

[28] M. Medhioub, I. Khanfir Kallel, S. Ammar Bouhamed, N. Derbel, B. Solaiman, O. Kanoun, Electronic embedded system for stair recognition based on possibilistic modeling of ultrasonic signal, IEEE Sensors Journal 21 (5) (2021-03) 5787–5797, conference Name: IEEE Sensors Journal. doi:10.1109/JSEN.2020.3035834.

[29] Y. Choudhary, N. Malhotra, P. K. Sahoo, S. Kamal, Data-driven modeling of a track-based stair-climbing wheelchair, in: 2021 IEEE/ASME International Conference on Advanced Intelligent Mechatronics (AIM), 2021, pp. 1000–1005, ISSN: 2159-6255. doi:10.1109/AIM46487.2021.9517494.

[30] S. Sivakanthan, J. Castagno, J. L. Candiotti, J. Zhou, S. A. Sundaram, E. M. Atkins, R. A. Cooper, Automated curb recognition and negotiation for robotic wheelchairs, Sensors 21 (23) (2021) 7810, number: 23 Publisher: Multidisciplinary Digital Publishing Institute. doi:10.3390/s21237810.
URL https://www.mdpi.com/1424-8220/21/23/7810

[31] B. Ramalingam, R. Elara Mohan, S. Balakrishnan, K. Elangovan, B. Félix Gómez, T. Pathmakumar, M. Devarassu, M. Mohan Rayaguru, C. Baskar, sTetro-deep learning powered staircase cleaning and maintenance reconfigurable robot, Sensors 21 (18) (2021) 6279, number: 18 Publisher: Multidisciplinary Digital Publishing Institute. doi:10.3390/s21186279.
URL https://www.mdpi.com/1424-8220/21/18/6279

[32] J. Chocoteco, R. Morales, V. Feliu, L. Sánchez, Trajectory planning for a stair-climbing mobility system using laser distance sensors, IEEE Systems Journal 10 (3) (2014) 944–956.

[33] J. Chocoteco, R. Morales, V. Feliu, Improving the climbing/descent performance of stair-climbing mobility systems confronting architectural barriers with geometric disturbances, Mechatronics 30 (2015) 11–26.

[34] R. Morales, A. Gonzalez, V. Feliu, P. Pintado, Environment adaptation of a new staircase-climbing wheelchair, Autonomous Robots 23 (4) (2007) 275–292.

[35] S. Nakajima, A new personal mobility vehicle for daily life: improvements on a new rt-mover that enable greater mobility are showcased at the cybathlon, IEEE Robotics & Automation Magazine 24 (4) (2017) 37–48.

Andrea Botta is a PhD student in Mechanical Engineering at Politecnico di Torino, Italy. He received his BSc in Mechanical engineering in Mechanical Engineering in 2014 and completed his MSc in Mechatronic Engineering in 2017, both at Politecnico di Torino. His research interest lies in the design and the development of innovative mobile service robots and assistive technologies. **Roberto Bellincioni** Roberto Bellincioni

is a master's degree holder in Mechanical Engineering at Politecnico di Torino, Italy. He received his BCs in Mechanical Engineering in 2017 and completed his MSc in Mechanical Engineering in 2020, both at Politecnico di Torino. **Giuseppe**

Quaglia is a full professor of Applied Mechanics at Politecnico di Torino His scientific activity, is mainly related to: energy Saving, renewable energy, and sustainability; vehicle dynamic and systems; robotics and mechatronics; automation, actuators, and mechanisms; device for disabled people and biomedical applications; appropriate technologies and systems for sustainable human development. He is: Deputy chair of IFToMM Italy (International Federation for the Promotion of Mechanism and Machine Science); Chair of Technical Committee for Sustainable Energy Systems of IFToMM; Member of SIRI council, (Italian Association of Robotics and Automation); Member of Management Board of "Politecnico Interdepartmental Center for Service Robotics" (PIC4SeR).

Appendix A. Autonomous climbing sequence

Figure A.9: Autonomous climbing sequence